Journal of Photochemistry & Photobiology, B: Biology 153 (2015) 233–239

Contents lists available at ScienceDirect

Journal of Photochemistry & Photobiology, B: Biology

journal homepage: www.elsevier.com/locate/jpb

Scavenging of photogenerated ROS by Oxicams. Possible biological and environmental implications

Gabriela V. Ferrari [a], José Natera [b], M. Paulina Montaña [a], Vanesa Muñoz [a], Eduardo L. Gutiérrez [a], Walter Massad [b], Sandra Miskoski [b], Norman A. García [b,*]

[a] Area de Química Física, Universidad Nacional de San Luis, 5700 San Luis, Argentina
[b] Departamento de Química, Universidad Nacional de Río Cuarto, 5800 Río Cuarto, Argentina

ARTICLE INFO

Article history:
Received 3 July 2015
Received in revised form 2 September 2015
Accepted 21 September 2015
Available online 28 September 2015

Keywords:
Oxicams
Photodegradation
Photoprotection
Photosensitization
Riboflavin
ROS

ABSTRACT

The profusely employed drugs Piroxicam (Piro), Tenoxicam (Teno) and Meloxicam (Melo) belonging to the non-steroidal antiinflammatory drug (NSAID) family of the Oxicams (Oxis) were studied in the frame of two specific conditions: (a) their ROS scavenging ability, in relation to a possible biological antioxidant action and (b) their photodegradability under environmental conditions, in the context of Oxi-contaminated waters.

Singlet molecular oxygen ($O_2(^1\Delta_g)$) and superoxide radical anion ($O_2^{\bullet-}$) were photogenerated through Riboflavin (Rf, vitamin B2)-photosensitization in aqueous and aqueous-methanolic solutions in the presence of Oxi concentrations in the range 50–500 μM. The visible-light absorber vitamin is currently present in all types of natural waters and constitutes the most frequent endogenous photosensitizer in mammals. Hence, it was employed in order to mimic both natural sceneries of interest.

All three Oxis quench $O_2(^1\Delta_g)$ with rate constants in the order of 10^8 M^{-1} s^{-1} showing a significant photodegradation efficiency given by a dominant reactive fashion for deactivation of the oxidative species. Although this is not a desirable property in the context of photoprotection upon prolonged photoirradiation, constitutes in fact a promissory aspect for the degradation NSAIDs, in waste waters. Indirect evidence indicates that Melo is also oxidized through a $O_2^{\bullet-}$-mediated component.

The simultaneous presence of Piro plus tryptophan or tyrosine under Rf-photosensitizing conditions, which has taken the amino acids as photooxidizable model residues in a proteinaceous environment, indicates that the NSAID induces a protection of the biomolecules against photodynamic degradation.

1. Introduction

The confirmation of the presence of oxidative markers, including reactive oxygen species (ROS) in human brain areas affected by neurodegenerative disorders (ND) immediately links both facts in a kind of cause–effect relationship [1,2].

Oxidative stress is highly aggressive to brain tissue, and an increased production of ROS may initiate the concomitant inflammatory response, commonly associated to ND [3]. Relatively recent research works suggest some connection degree between a retardation in ND manifestation and prolonged administration of anti-inflammatory medicaments, such as non-steroidal antiinflammatory drugs (NSAIDs) [4,5]. In short, it is currently accepted that NSAIDs could play a protective role in ND.

In this context, we decided to carry out an in vitro research work, in order to know more on the possible action of several families of NSAIDs as protectors against ROS-mediated deterioration of biological targets. We started with a study on two NSAIDs: the salicylic acid derivative Diflunisal and the indolic-acid derivative Indomethacin [6]. In the present contribution our interest is directed to the hydroxy-aromatic NSAID family of the Oxicams (Oxis). Three members of this family, named Piroxicam (Piro), Tenoxicam (Teno) and Meloxicam (Melo) were selected for the study. Their respective structural formulae are given below (Scheme 1).

Regarding the possible beneficial effects of Oxi on ND, several researchers published a series of results on the protective action of the NSAIDs against different oxidative agents [7,8,9,10]. Nevertheless, it should be emphasized that NSAIDs also induce a number of adverse side effects [11]. As an example, the mentioned Oxi derivative causes some undesired reactions such as photosensitivity and gastropathies; the latter is a common characteristic present in several NSAIDs [12, 13].

As a second objective of our study, in line with an eventual Oxi–ROS interaction, is the evaluation of the chemical resistance of NSAIDs under photoirradiation in simulated natural/environmental conditions. Pharmaceutically active substances, and very specially NSAIDs, are a class of urban water-contaminants – presently mentioned as *emerging contaminants* – that have increased their health concern in the last years [14,15]. On these grounds, a number of studies were directed to

* Corresponding author.
E-mail address: ngarcia@exa.unrc.edu.ar (N.A. García).

http://dx.doi.org/10.1016/j.jphotobiol.2015.09.024
1011-1344/

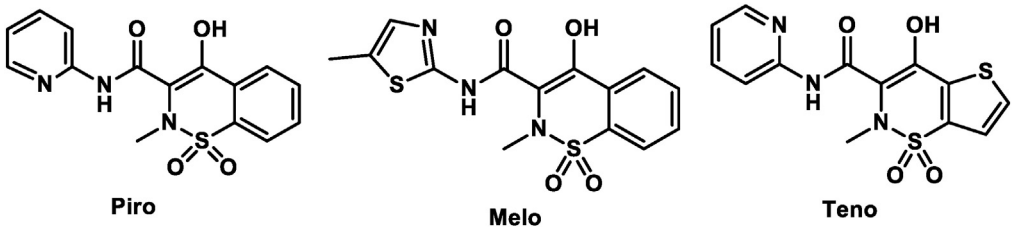

Scheme 1. Chemical structures of Piroxicam (Piro), Meloxicam (Melo) and Tenoxicam (Teno).

investigate the naturally-induced degradation of different families of NSAIDs, in particular through ROS-mediated photochemical ways [16,17]

There is a moderate amount of literature dealing with the scavenging of oxidative species by Oxi. Van Antwerpen and Nève reported an important interaction of Oxi with hypochlorous acid whereas it was low with hydroxyl radical and not observable with hydrogen peroxide (H_2O_2) [18]. Günther et al. studied the scavenging of $O_2(^1\Delta_g)$ by Piro and Teno. The Oxi resulted good quenchers of the oxidative species [19,20]. More recently Salat et al. observed the effect of Oxi against nitro-oxidants and Amzoiu et al. and Santiago et al. demonstrated the increase of SOD activity provoked by Oxi in different bioassays [8,9,10].

In the present work, the ROS were photogenerated in the presence of Oxi, employing specifically Riboflavin (Rf, vitamin B2) as a photosensitizer. The vitamin was chosen for that purpose because it is a naturally occurring endogenous compound of singular importance. It is present in practically all living organisms and surface waters, and it is a well known sensitizer for the light-promoted oxidation of biologically and environmentally interesting substrates [21,22].

Since Rf and Oxi may occupy common locations in complex biological structures and surface waters, kinetic and mechanistic information can help to understand the behavior of Oxy towards Rf-generated ROS, the potential in-vivo consequences and the propensity of such processes to occur under given environmental conditions. In a parallel work, the amino acids (AAs) tryptophan (trp) and tyrosine (tyr) were employed as typical oxidizable targets in a proteinaceous medium, in order to evaluate an eventual antioxidant/protective effect of the Oxi towards biologically relevant substrates.

The information reported in this paper may be of great concern in pharmaceutical, medical and toxicological fields, especially for getting insight into the effectiveness and extent of possible photobiological processes in the presence of natural daylight-absorbing substances.

2. Experimental section

2.1. Chemicals

Piroxicam [4-hydroxy-2-methyl-N-(pyridin-2-yl)-2H-1,2-benzothiazine-3-carboxamide1,1-dioxide] (Piro), Meloxicam [4-hydroxy-2-methyl-N-(5-methyl-2-thiazolyl)-2H-1,2-benzothiazine-3-carboxamide 1,1-dioxide] sodium salt (Melo) and Tenoxicam [4-hydroxy-2-methyl-N-(pyridin-2-yl)-/2H-thieno (2,3-e)-1,2 thiazine-3-carboxamide 1,1-dioxide] (Teno), Riboflavin, Rose Bengal (RB), sodium azide (NaN_3), superoxide dismutase (SOD) from bovine erythrocytes, L-tryptophan (trp) and L-tyrosine (tyr) were purchased from Sigma Chem. Co. Furfuryl alcohol (FFA) was from Riedel de Haën. Deuterated water (D_2O, 99.9% D) and monodeuterated methanol (MeOD) were both from Sigma Chem. Co. whereas methanol (MeOH) HPLC quality was provided by from Sintorgan. Water was triply distilled. Phosphate buffer was employed in the regulation of pH/pD. D_2O and MeOD were employed in the time-resolved determinations of $O_2(^1\Delta_g)$ phosphorescence emission, in order to enlarge the lifetime of this species.

Due to solubility reasons pH 7 buffered H_2O or buffered D_2O was employed for Melo and a mixture of pH 7 buffered H_2O–MeOH 1:1 (v/v) or buffered pD 7 D_2O–MeOD 1:1 (v/v) for Teno and Piro.

2.2. Instrumentation and methods

Stationary Rf fluorescence experiments were carried out in a RF 5301-PC Shimadzu spectrofluorometer at 25 ± 1 °C in air equilibrated solutions. The respective excitation and emission wavelengths were 445 and 515 nm. Ground state absorption spectra were registered in a Hewlett Packard 8452A diode array spectrophotometer. Stationary aerobic photolysis of sensitizer + Oxi solutions was carried out in a home-made photolyzer for non-monochromatic irradiation (150 W quartz-halogen lamp), using a cut-off filter of 480 or an interference filter of 450 nm in order to ensure that the light was only absorbed by the sensitizers.

The rates of sensitized photooxygenation of Oxi were determined from the initial slopes of the plots of Oxi consumption vs. irradiation time. The substrate consumption was monitored from absorbance decay of the respective *maxima* of the Oxi, in the range of 350–370 nm.

The rates of oxygen uptake were determined employing a selective oxygen electrode (Orion 97-08) as already described elsewhere (approximate response time 3 s/ppm and ±0.05 ppm accuracy) [6].

The reactive rate constant, k_r, for the reaction of $O_2(^1\Delta_g)$ with Oxi was determined as described in the literature, employing FFA as a reference compound (R) with $k_{rR} = 2.1 \cdot 10^8\ M^{-1}\ s^{-1}$ [23].

Time-resolved phosphorescence detection of $O_2(^1\Delta_g)$ was carried out with a laser-kinetic spectrophotometer previously described [24] employing RB with A_{532} ca. 0.5 as a sensitizer. All decay kinetics were the first order.

All experimental work was made at RT.

3. Results

It is worth mentioning that Oxi can exist in different states of aggregation, tautomerism and ionization, depending on the characteristic and pH of the solvent [25,26]. We have chosen the pH 7-aqueous solution as working medium. In it, the NSAIDs mainly remain as monomeric anionic species, with the OH group in position 4 deprotonated [27].

3.1. Stationary photolysis

Fig. 1 shows the changes in the absorption spectrum after irradiation of a pH 7 aqueous solution containing 50 μM Rf plus 55 μM Melo solution. From parallel experiments of the same described solution, oxygen uptake was observed. In both experiments similar qualitative results were obtained for the three Oxis examined. Relative values (RR_{Rf}) for the rates of Oxi consumption are shown in Table 1.

The described results strongly suggest that under 450 nm-photoirradiation of the mixture Rf–Oxi, the overall Oxi degradation includes the involvement of electronically excited states of the pigment with possible participation of ROS. On this basis, we developed a systematic kinetic study in order to elucidate the mechanism responsible for the Rf sensitized degradation of Oxi.

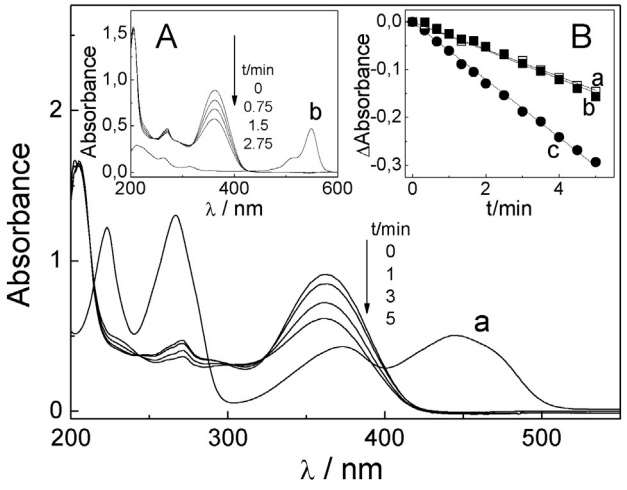

Fig. 1. Changes in the UV–vis absorption spectra of 50 μM Rf plus 55 μM Melo vs. 50 μM Rf upon photoirradiation (λ_{irr} = 450 nm interference filter). The trace a is the absorption spectrum of 50 μM Rf vs. solvent; inset A: changes in the UV–vis absorption spectra of 52 μM RB plus 55 μM Melo vs. 52 μM RB upon photoirradiation (λ_{irr} > 480 nm, cut off filter). The trace b is the absorption spectrum of 50 μM RB vs. solvent; inset B: Oxi consumption vs. irradiation time (λ_{irr} > 480 nm, cut off filter) in solutions containing 50 μM Rf plus 0.5 mM Teno (a); 0.5 mM Piro (b) and 0.5 mM Melo (c). In all cases under air saturated conditions. Solvents: aqueous buffer pH 7 for Melo and MeOH–H_2O (buffer pH 7), 1:1 v/v for Teno and Piro.

The final evaluation of the whole experimental results described in this section indicates the occurrence of the mechanistic steps represented in Scheme 2, later discussed. Nevertheless the scheme is displayed now in order to adequately identify in the text the involved kinetic steps and the different abbreviations employed.

$^1Rf^*$, $^3Rf^*$ and $O_2(^3\Sigma_g^-)$ represent the electronically excited singlet and triplet states of Rf and ground state molecular oxygen, respectively, whereas O_2•−, $O_2(^1\Delta_g)$ and Pn are the species superoxide radical anion, singlet molecular oxygen and eventual products for each corresponding (n) reaction, respectively.

3.2. Quenching of Rf electronically excited states

The presence of Oxi in the mM concentration range produces fluorescence quenching of Rf, as determined by stationary measurements. Through the monitoring of fluorescence intensity of the vitamin in the presence (I_f) and in the absence (^0I_f) of different Oxi concentrations (Fig. 2), the Stern–Volmer treatment ($^0I_f / I_f = 1 + {}^1K_{SV}$ [Oxi], with $^1K_{SV} = {}^1k_q \cdot {}^1\tau_o$) allows the determination of the Stern–Volmer ($^1K_{SV}$) constant. The rate constant ^1k_q accounts for process (2) and τ_o = 5.6 ns is the reported value for the fluorescence lifetime of $^1Rf^*$ [28]. The obtained rate constants ^1k_q are shown in Table 1.

It is known that the anaerobic visible light-mediated degradation of Rf in solution, in the absence of oxygen, proceeds through $^3Rf^*$ for which a lifetime ($^3\tau_0$) of 15 μs has been reported [29,30]. The rate of the process ($Rate_{Rf}$) is currently estimated through the absorbance decrease in the Rf absorption spectrum, monitored at 445 nm as a function of irradiation time (Fig. 2, inset). In the individual presence of 0.4 mM Melo; 0.6 mM Teno and 0.4 mM Piro, the rate of Rf decomposition ($Rate_{Rf\ +\ Oxi}$) decreased 90% for Melo, 94% for Teno and 95% for Piro as compared to the rate in the absence of the Oxi. The experimental data strongly supports the idea that the long-lived intermediary in the photolysis, represented by the electronically excited triplet state of the vitamin, is efficiently quenched by relatively low Oxi concentrations. From the evaluation of the ratios of respective rates of Rf decomposition in the absence and in the presence of the NSAIDs and through a Stern–Volmer treatment ($Rate_{Rf} / Rate_{Rf\ +\ Oxi} = 1 + {}^3k_{q\ app}\ {}^3\tau_0$ [Oxi]) the apparent rate constant values ($k_{q3\ app}$), accounting for the quenching of $^3Rf^*$ by the Oxi can be roughly calculated (Table 1). The estimated error for $^3k_{q\ app}$ values was ±25%.

$$Rf + h\nu \longrightarrow {}^1Rf^* \longrightarrow {}^3Rf^* \quad (1)$$

$$^1Rf^* + Oxi \longrightarrow Rf + Oxi \text{ or } P2 \quad \text{Rate constant } {}^1k_q \quad (2)$$

$$^3Rf^* + O_2(^3\Sigma_g^-) \longrightarrow Rf^{\bullet+} + O_2^{\bullet-} \quad (3)$$

$$^3Rf^* + Oxi \longrightarrow Rf^{\bullet-} + Oxi^{\bullet+} \quad \text{Rate constant } {}^3k_{q\ app} \quad (4)$$

$$Rf^{\bullet-} + H^+ \longrightarrow RfH^\bullet \quad (5)$$

$$2\ RfH^\bullet \longrightarrow Rf + RfH_2 \quad (6)$$

$$RfH_2 + O_2(^3\Sigma_g^-) \longrightarrow RfH_2^{\bullet+} + O_2^{\bullet-} \quad (7)$$

$$O_2^{\bullet-} + Oxi \longrightarrow P8 \quad (8)$$

$$^3Rf^* + O_2(^3\Sigma_g^-) \longrightarrow Rf + O_2(^1\Delta_g) \quad (9)\ \text{Rate constant } k_{ET}$$

$$O_2(^1\Delta_g) \longrightarrow O_2(^3\Sigma_g^-) \quad (10)\ \text{Rate constant } k_d$$

$$O_2(^1\Delta_g) + Oxi \longrightarrow O_2(^3\Sigma_g^-) + Oxi \quad (11)\ \text{Rate constant } k_q$$

$$O_2(^1\Delta_g) + Oxi \longrightarrow P12 \quad (12)\ \text{Rate constant } k_r$$

being $k_t = k_r + k_q$

Scheme 2. Possible reaction pathways in the Rf-sensitized photooxidation of Oxicams.

3.3. Interaction of Oxi with photogenerated ROS

To describe the photooxidation processes in aerobic Rf-sensitized events in solution, the participation of the species O_2•−, reaction (3), generated by electron transfer with quantum yield ΦO_2•− = 0.009 and $O_2(^1\Delta_g)$ produced by energy transfer with quantum yield Φ_Δ = 0.47, reaction (9) have been demonstrated [31,32].

In order to test the potential participation of $O_2(^1\Delta_g)$ and O_2•− in the Rf-photosensitized degradation of Oxi, oxygen consumption experiments were performed. The rates of oxygen consumption (ROU) were determined in the presence and in the absence of 1 μg/ml SOD, and 1 mM NaN_3, specific O_2•− and $O_2(^1\Delta_g)$ interceptors, in solutions containing 40 μM Rf and 0.5 mM Oxi.

Table 1
Rate constant for the quenching of singlet excited state of Rf (^1k_q) and apparent rate constant for the quenching of triplet excited state of Rf and ($^3k_{q\ app}$); rate constants for the overall and reactive quenching of $O_2(^1\Delta_g)$ (k_t and k_r), k_r / k_t ratio and relative rates of Oxi consumption upon Rf (RR_{Rf}) and RB (RR_{RB}) photosensitization. Solvents: aqueous buffer pH 7 for Melo and MeOH–H_2O buffer pH 7, 1:1 v/v for Teno and Piro.

Compound	^1k_q 10^{10} M^{-1} s^{-1}	$^3k_{q\ app}$ 10^9 M^{-1} s^{-1}	k_t 10^8 M^{-1} s^{-1} (a)	k_r 10^8 M^{-1} s^{-1}	k_r/k_t	RR_{Rf}	RR_{RB}
Meloxicam (Melo)	2.84 ± 0.12	1.5 ± 0.3	1.15 ± 0.06	0.73 ± 0.04	0.63	1	1
Piroxicam (Piro)	0.88 ± 0.04	1.9 ± 0.4	1.00 ± 0.07 (1.1) (b)	0.50 ± 0.03 (0.61) (b)	0.52	0.48	0.68
Tenoxicam (Teno)	2.3 ± 0.06	1.7 ± 0.3	0.49 ± 0.05	0.48 ± 0.06 (1.6) (c)	~1	0.47	0.67

(a) D_2O pH 7 for Melo and MeOH–D_2O (pD 7) 1:1 v/v for Teno and Piro.
(b) In dioxane–water (molar fraction of water = 0.91) [19]. (e) In MeCN [20].

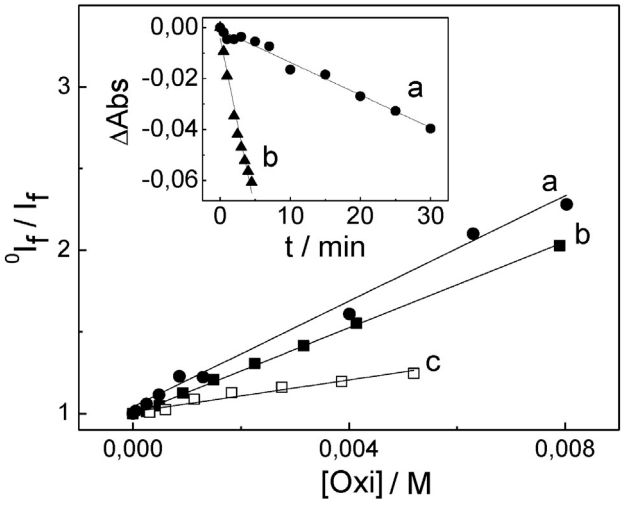

Fig. 2. Stern–Volmer plots for the determination ^1k_q of Melo (a), Teno (b) and Piro (c). Inset: absorbance decrease, monitored at 445 nm, as a function of irradiation time ($\lambda_{irr} > 480$ nm, cut off filter) for deaerated pH 7 buffered aqueous solutions of 50 μM Rf in the absence (a) and in the presence (b) of 0.43 mM Melo. Solvents: aqueous buffer pH 7 for Melo and MeOH–H_2O (buffer pH 7), 1:1 v/v.

The enzyme SOD, that dismutates $O_2^{\bullet-}$ as shown in reaction (13), has been employed to confirm or discard the participation of that species in a given oxidative event [33].

$$2O_2^{\bullet-} + 2H^+ + SOD \rightarrow O_2(^3\Sigma_g^-) + H_2O_2 \quad (13)$$

Results constitute the mean values of three runs that do not differ in more than 3% and are shown in Fig. 3. The presence of SOD produces an increase in the ROU of Piro and Teno and a decrease in the case of Melo.

Although SOD is a recognized quencher of $O_2(^1\Delta_g)$ [34], the possibility that in the stationary irradiation experiments, the ROU were increased due to an eventual $O_2(^1\Delta_g)$-mediated oxidation of protein, must be disregarded. Our results show that the phosphorescence lifetime of $O_2(^1\Delta_g)$ in MeOD–D_2O 1:1 (v/v) remains the same in the presence and in the absence of 1 μg/ml SOD.

The presence of NaN_3 reduces in a 60–80% the individual ROU of all three Oxy, as compared to the respective ROU in the absence of the salt (data not shown). It is known that NaN_3 physically quenches $O_2(^1\Delta_g)$, with a rate constant $k_q = 4.5\ 10^8$ in pH 7 water (Eq. (11) with NaN_3 instead of Oxi) [35].

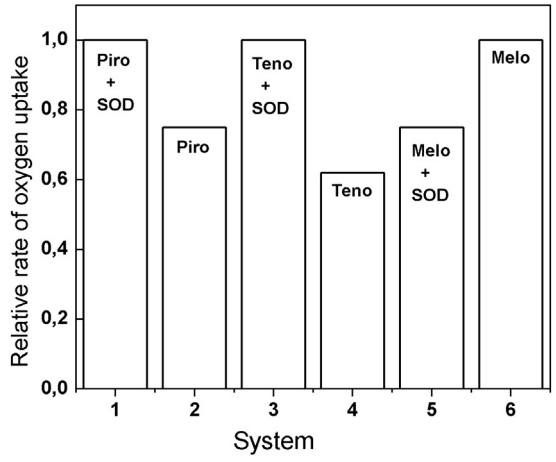

Fig. 3. Relative rates of oxygen uptake upon photoirradiation ($\lambda_{irr} > 480$ nm, cut off filter) of: 50 μM Rf + 0.5 mM Piro in the presence (1) and in the absence of 1 μg/ml SOD (2); 50 μM Rf + 0.5 mM Teno in the presence (3) and in the absence of 1 μg/ml SOD (4); 50 μM Rf + 0.5 mM Melo in the presence (5) and in the absence (6) of 1 μg/ml SOD. Solvents: aqueous buffer pH 7 for Melo and MeOH–H_2O (buffer pH 7), 1:1 for Teno and Piro.

Regarding the possible interaction Oxi–$O_2(^1\Delta_g)$, Rose Bengal (RB), a well-known exclusive generator of the oxidative species, was employed as a photosensitizer [36]. It was chosen in order to focus the potential reaction of Oxi on the $O_2(^1\Delta_g)$-mediated process, eliminating possible interferences due to interactions of the NSAIDs with Rf electronically excited states and/or with other ROS different from $O_2(^1\Delta_g)$.

When individual Oxi solutions, in the presence of 53 μM RB, were photoirradiated, modifications in the Oxi spectral component, very similar to each other for the three derivatives, were observed (see Fig. 1, inset, for a typical case). Relative rates of 0.5 mM Oxi consumption upon RB-photosensitization (RR_{RB}) were collected in Table 1, for comparative purposes.

Employing RB for the generation of $O_2(^1\Delta_g)$ in the TRPD experiments, the phosphorescence decay kinetics was the first order. The individual presence of the Oxi in the mM concentration range leads to a decrease in the lifetime of the oxidative species, confirming the interaction Oxi–$O_2(^1\Delta_g)$. Through the Stern–Volmer treatment $\tau_{\Delta o} / \tau_\Delta = 1 + k_t \tau_{\Delta o}$ [Oxi], where τ_Δ and $\tau_{\Delta o}$ are the $O_2(^1\Delta_g)$ phosphorescence lifetimes in the presence and in the absence of Oxi respectively, the k_t values were obtained. The rate constant k_t accounts for the overall interaction Oxi–$O_2(^1\Delta_g)$ (see Scheme 2, bottom). Results are shown in Table 1.

Through the monitoring of the respective rates of Oxi consumption upon RB-sensitized photoirradiation, the rate constants for reactive interaction Oxi–$O_2(^1\Delta_g)$ (k_r, process (12) with [Oxi] = 55 μM), were obtained. RB was employed as a dye sensitizer ($A_{560} = 0.4$) and FFA was the reference compound. The first order plots employed for the determination of k_r are shown in Fig. 4 and the respective rate constant values are included in Table 1. In the same Table appears the particularly useful information represented by the k_r/k_t ratio, accounting for the fraction of overall quenching of $O_2(^1\Delta_g)$ by the substrate that effectively leads to a chemical transformation.

3.4. Comparative experiments on the photooxidation rates of tryptophan and tyrosine in the presence of Piroxicam

The possible activity of Oxi as protectors against photodamage of proteins was evaluated by employing the AAs trp and tyr as oxidizable targets in the presence of Rf and light. Both AAs belong to the group of

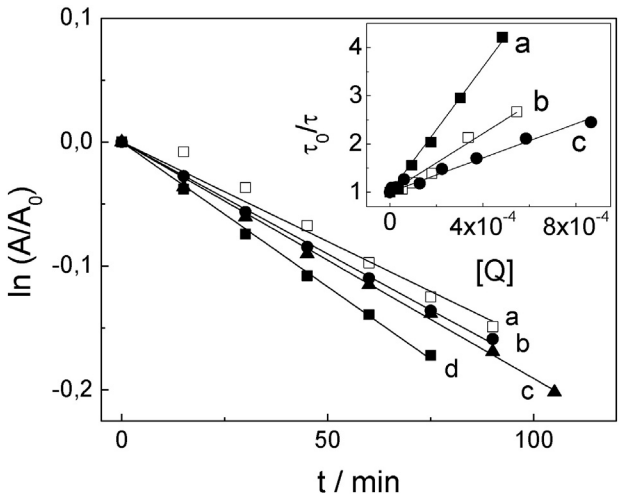

Fig. 4. First order plots for substrate consumption of 53 μM Rose Bengal plus 0.5 mM: Teno (a); Piro (b); Melo (c) and FFA (d) upon photoirradiation ($\lambda_{irr} > 480$ nm, cut off filter). Solvents: aqueous buffer pH 7 for Melo and MeOH–H_2O (buffer pH 7), 1:1. Inset: Stern–Volmer plot for the quenching of $O_2(^1\Delta_g)$ phosphorescence by Melo (a); Piro (b) and Teno (c). Solvents: D_2O buffer pD 7 for Melo and MeOD–D_2O buffer pD 7, 1:1 v/v for Teno and Piro.

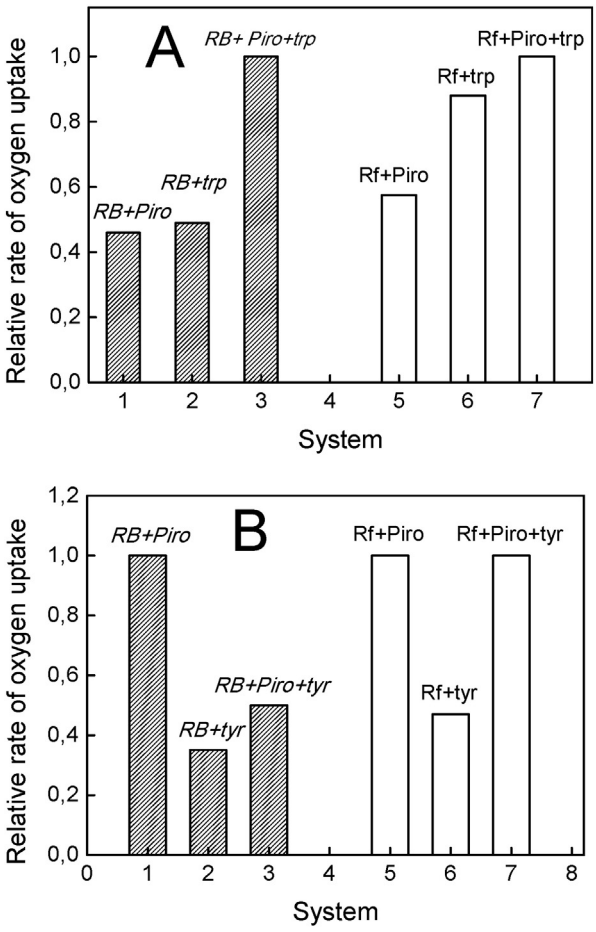

Fig. 5. Panel A. Dashed bars: relative rate of oxygen uptake by of 50 μM RB in the presence of 0.5 mM Piro (1); 0.5 mM trp (2) and 0.5 mM Piro plus 0.5 mM trp. Empty bars: relative rate of oxygen uptake by of 45 μM Rf in the presence of 0.5 mM Piro (1); 0.5 mM trp (2) and 0.5 mM Piro plus 0.5 mM trp. Panel B. Dashed bars: relative rate of oxygen uptake by of 50 μM RB in the presence of 0.5 mM Piro (1); 0.5 mM tyr (2) and 0.5 mM Piro plus 0.5 mM tyr. Empty bars: relative rate of oxygen uptake by of 45 μM Rf in the presence of 0.5 mM Piro (1); 0.5 mM tyr (2) and 0.5 mM Piro plus 0.5 mM tyr. Solvents: aqueous buffer pH 7 for Melo and MeOH–H_2O (buffer pH 7), 1:1 for Teno and Piro. In all cases (panels A and B) $\lambda_{irr} > 480$ nm, cut off filter.

protein fractions that are affected by photodamages through photodynamic activity [37]. In this case, Rf plays the role of a naturally occurring ROS-photogenerator.

The ROU in photoirradiated individual solutions of 0.5 mM of the amino acids (AAs) trp and tyr plus 45 μM Rf were evaluated in the absence and in the presence of 0.5 mM Piro. The respective rates (Fig. 5) can be considered as a measure of the overall photooxidability of each system under the established experimental conditions. Piro was chosen for this part of the study because it presents intermediate kinetic values in the photooxidation experiments (Table 1).

4. Discussion

4.1. The interaction of Oxi with $^1Rf^*$ and $^3Rf^*$

Teno, Melo and Piro interact with $^1Rf^*$ and $^3Rf^*$. Nevertheless, according to fluorescence quenching data, Oxi concentrations in the sub-mM range, like those employed in this work, are not enough to intercept $^1Rf^*$. Hence, the participation of $^1Rf^*$ in a photodegradative pathway must be disregarded.

On the other hand, experimental evidence strongly supports the quenching of $^3Rf^*$ by the Oxi. The quenching represented by Eq. (4) starts a cascade of radical-mediated photoreactions that include Oxi photodegradation and possible generation of ROS.

4.2. The interaction of Oxi with ROS

Results in the Rf-photosensitized experiments, in the presence of specific interceptors of ROS suggest, in principle, the participation of several ROS in the oxidative events. As said, the quantum yield for direct $\Phi O_2^{\bullet -}$ production through reaction (3) is extremely low and must be neglected. In practical terms, the species $O_2^{\bullet -}$ should appear, in a significant fashion, after the radical-generator step (4). Its production is competitive with $O_2(^1\Delta_g)$ production (step (12)), and the prevalence of some of these pathways will depend on the rate constant values $^3k_{q\ app}$ and k_{ET} and the respective Oxi and dissolved $O_2(^3\Sigma_g^-)$ concentrations. On the basis that the k_{ET} value of process (12) in MeOH–H_2O (1×10^8 M^{-1} s^{-1}, i.e., 1/9 of the diffusional value) [38] and a mean $^3k_{q\ app}$ value for the Oxi of 1.7×10^9 M^{-1} s^{-1} (Table 1), it can be deduced that, for the same concentrations of Oxi and dissolved $O_2(^3\Sigma_g^-)$, processes (4) and (12) occur with a are very close rate.

In thermodynamic terms, the viability of the electron transfer process (4), is typically assessed by means of the Gibbs free energy for electron transfer, $\Delta_{ET}G_0 = E_{0(Oxi/Oxi+)} - E_{0(Rf/Rf-)} - E_{Rf^*} + C$; being $E_{0(Oxi/Oxi+)}$ 0.60 V; 0.74 V and ca. 0.65 V for Melo, Teno and Piro respectively, [39,40,41] the electrode potentials of the electron donor, $E_{0(Rf/Rf-)}$ is the standard electrode potential of the acceptor Rf (−0.80 V), E_{Rf^*} is the $^3Rf^*$ energy (2.17 eV), and C is the coulombic energy term (−0.06 V) [42]. $\Delta_{ET}G_0$ values of −0.83 V; −0.69 V and −0.78 for Melo, Teno and Piro respectively, indicate the feasibility of process (4). Consequently the species $O_2^{\bullet -}$ may be formed.

The increase of the ROU due to the presence of SOD for Teno and Piro and the decrease in the case of Melo can be due to the involvement of the species $O_2^{\bullet -}$, performing different mechanistic roles. Although a delay in the ROU in the presence of SOD should be in principle the expected effect for a $O_2^{\bullet -}$-mediated oxidation due to the inhibitory effect of reaction (13), the enzyme can either promote or restrain that oxidation. It has been shown that SOD stimulates oxidative processes on some phonolic-type substrates such as hydroquinones and gallic acid [43]. In these cases, in principle assimilable to those of Piro and Teno, the H_2O_2 produced in the dismutation reaction (13) could be the oxidative species through reaction (14).

$$H_2O_2 + Oxi \rightarrow P14 \quad (14)$$

Nevertheless, this reaction pathway has been already disregarded for Teno, Melo and Piro as already mentioned [18]. We think that in our case, the regeneration of $O_2(^3\Sigma_g^-)$ by SOD through reaction (13), at the expense of the species $O_2^{\bullet -}$, increases the production of the $O_2(^1\Delta_g)$ which reacts with Teno and Piro, increasing the ROU.

The effect of SOD, decreasing the ROU for Melo – the most oxidizable derivative among the studied Oxi, according to the oxidation potential values – indicates an effective interaction Melo–$O_2^{\bullet -}$ (reaction (8)). In synthesis, the conjunctive operation of reactions (1) + (14) + (12) rationalizes the observed increase in ROU by Teno and Piro in the presence of SOD, whereas reaction (8) justifies the observed delay in the case of Melo.

The quenching of $O_2(^1\Delta_g)$ by Oxi was clearly demonstrated through the TRPD experiments. According to our knowledge, the only reports on rate constant values for the interaction belong to Lemp and Günther and Günther et al. [19,20]. These values, determined in MeCN and H_2O–dioxane mixtures are in the range of those obtained in the present work, and have been incorporated to Table 1 for comparative purposes.

Both the respective k_t and k_r values in our work are within those typically expected for hydroxyl-aromatic derivatives, where the ionized OH-group enhances the effective $O_2(^1\Delta_g)$-mediated photooxidation (reaction (12)) [35,44]. The considerably high values for the quotient k_r/k_t exhibited by the Oxi (Table 1) are, in the present case, an unwanted

quality, in the context of the Oxi as ROS scavengers. The case of Teno constitutes the extreme example, for which every quenching event produces the degradation of the scavenger ($k_r/k_t \sim 1$, Table 1). On the other hand, the same quality is a promising result from the perspective of the visible-light-induced photodegradation of environmental pollutants, constituted in the present case by the Oxi family.

From the comparison of the respective relative rates of Oxi consumption RR_{RB} and RR_{Rf} shown in Table 1, several points are evident: in both cases Melo is the most degradable compound and the photodegradation rates for Teno and Piro are substantially lower and similar to each other. Further, the RR_{RB} values for Teno and Piro are lower than the corresponding RR_{Rf} ones. The last point can be rationalized by considering that Teno and Piro are preponderantly degraded through a $O_2(^1\Delta_g)$-mediated mechanism whereas a $O_2^{\bullet-}$-mediated component seems to operate simultaneously in the case of Melo, only for the Rf-sensitization.

4.3. Effect of Piro on the photooxidation of trp and tyr

The employment of the mixtures of Piro plus trp and tyr in the Rf-photosensitized experiments can be considered as a model system, roughly mimicking a natural bio-scenery. Kinetic information, in particular the overall ROU, may provide useful information accounting for understanding the potential protection of Oxi to proteinaceous residues towards photopromoted oxidation. The same experiments using RB as a photosensitizer may facilitate this interpretation, on the basis of the prevalent operation of $O_2(^1\Delta_g)$-mediated mechanism, as already mentioned.

The AAs trp and tyr are recognized quenchers of $^3Rf^*$ with rate constant values ^3k_q (reaction (4) with AA instead of Oxi) of $2.5 \times 10^9\ M^{-1}\ s^{-1}$ and $1.0 \times 10^9\ M^{-1}\ s^{-1}$ respectively [45]. The primary products are the reduced flavin radicals and the overall reaction observed was conversion of oxygen via $O_2^{\bullet-}$, which in turn reacts with the AAs [46].

Besides, the interaction of trp, and tyr with $O_2(^1\Delta_g)$ is well characterized, with reported rate constant values of $k_t = 7.2 \times 10^7\ M^{-1}\ s^{-1}$ and $k_r = 4.7 \times 10^7\ M^{-1}\ s^{-1}$ for the case of trp and $k_t = 1.5 \times 10^7\ M^{-1}\ s^{-1}$ in the case of tyr [45,46]. The phenolic AA is scarcely reactive in neutral pH medium and most of the interaction with $O_2(^1\Delta_g)$ must be ascribed to a physical deactivation of the oxidative species [44, 35].

As can be appreciated from Fig. 5A, employing RB as a dye sensitizer, the ROU for the mixtures trp–Oxi constitute the simple addition of the ROU values for the AA and Oxi individually considered. This fact can obey to the operation of a pure $O_2(^1\Delta_g)$-mediated mechanism and to the similitude of the rate constant values for the AAs and Piro. In the case of tyr, the RB photosensitization set shown in Fig. 5B presents a neat decrease in the ROU by the mixture Oxi + AA as compared to the one for the isolated Oxi. This can be due to the very low k_r/k_t exhibited by tyr, for which largely predominates the physical deactivation of the oxidative species [35].

The picture is some different with Rf as a photosensitizer. Piro and trp are efficient chemical scavengers of $O_2(^1\Delta_g)$, with practically the same k_r and very similar k_r/k_t values, when isolated. In parallel, the ROU for the mixture are much lower than the addition of the respective rates for trp and Piro. The possible reason for this fact could be attributable to the quenching of $^3Rf^*$ by the mixture Piro + trp. Both substrates exhibit relatively high ^3k_q values, and the pair could decrease by this way the stationary concentration of $O_2(^1\Delta_g)$ with the concomitant reduction of the overall ROU by the mixture. In the case of tyr, the ROU by the mixture is the same as that determined by the isolated Oxi. The relative increase in the ROU component by isolated tyr, so as in the case of trp, could be attributed to the contribution of a $O_2^{\bullet-}$-mediated pathway as mentioned earlier in this section.

An important overall result for both AAs employing Rf as dye sensitizer is that the overall ROU by the mixture Oxi + AA is lower than the corresponding addition of the rates for the individual components. This fact implies a positive sort of protection of the involved couple against in situ-photogenerated ROS.

5. Conclusions

The Oxi derivatives Teno, Piro and Melo dissolved in aerated aqueous solution, efficiently quench photogenerated $O_2(^1\Delta_g)$. Besides Melo, the most oxidizable derivative of the series, also interacts with $O_2^{\bullet-}$. Results may be usefully interpreted in connection to two natural sceneries:

(a) The ability of Oxi as effective scavengers of the in situ-generated $O_2(^1\Delta_g)$ constitutes an interesting property in the context of biomolecules protection.
(b) In Oxi-contaminated waters, the pollutants may be effectively photooxidized in the presence of visible-light-absorbers able to generate $O_2(^1\Delta_g)$.

The Oxis here studied belong to the so-called *sacrificial scavengers*, provided that these are degraded through the quenching process, concomitantly decreasing their active concentration against ROS. This characteristic makes Piro, Melo and especially Teno, good candidates for environmental photodegradation of waste waters. The photosensitizer pigment Rf is present as traces as in practically all kinds of water courses [47].

Acknowledgments

Financial support from Consejo Nacional de Investigaciones Científicas y Técnicas (CONICET), Secretaría de Ciencia y Técnica of the Universidad Nacional de Río Cuarto (SECyT UNRC) and Secretaría de Ciencia y Técnica of the Universidad Nacional de San Luis (SECyT UNSL), all from Argentina, is grateful acknowledged.

References

[1] E.G. McGeer, P.L. McGeer, Inflammatory processes in Alzheimer disease, Prog. Neuropsychopharmacol. 27 (2003) 741–749.
[2] M. Dumont, M. Flint Beal, Neuroprotective strategies involving ROS in Alzheimer disease, Free Radic. Biol. Med. 51 (2011) 1014–1026.
[3] A.D. Roth, G. Ramírez, R. Alarcón, R. Von Bernhardi, Oligodendrocytes damage in Alzheimer's disease: beta amyloid toxicity and inflammation, Biol. Res. 38 (2005) 381–387.
[4] E. Esposito, V. Di Matteo, A. Benigno, M. Pierucci, G. Crescimanno, G. Di Giovanni, Non-steroidal anti-inflammatory drugs in Parkinson's disease, Exp. Neurol. 205 (2007) 295–312.
[5] A. Arfi, M. Richard, C. Gandolphe, D. Bonnefont-Rousselot, P. Thérond, D. Scherman, Neuroinflammatory and oxidative stress phenomena in MP S IIIA mouse model: the positive effect of long-term aspirin treatment, Mol. Genet. Metab. 103 (1) (2011) 18–25.
[6] R. Purpora, W. Massad, G. Ferrari, E. Reynoso, S. Criado, S. Miskoski, A. Pajares, N.A. García, The NSAIDs Indomethacin and Diflunisal as scavengers of photogenerated reactive oxygen species, Photochem. Photobiol. 89 (2013) 1463–1470.
[7] N. Vartiainen, C.Y. Huang, A. Salminen, G. Goldsteins, P.H. Chan, J. Koistinaho, Piroxicam and NS-398 rescue neurones from hypoxia/reoxygenation damage by a mechanism independent of cyclo-oxygenase inhibition, J. Neurochem. 76 (2) (2001) 480–489.
[8] K. Salat, A. Moniczewski, T. Librowski, Nitrogen, oxygen or sulfur containing heterocyclic compounds as analgesic drugs used as modulators of the nitroxidative stress, Mini Rev. Med. Chem. 13 (2013) 335–352.
[9] D.-C. Amzoiu, C. Pisoschi, C.A. Stănciulescu, M. Beznă, F. Popescu, G. Rău, Blood superoxide dismutase activity in patients with knee osteoarthritis treated with Oxicams, Farmacia 62 (2014) 460–466.
[10] R.M. Santiago, J. Barbiero, B.J. Martinhak, S.L. Boschen, L.M. da Silva, M.F.P. Werner, C. Da Cunha, R. Andreatini, M.M.S. Lima, M.A.V.F. Vital, Antidepressant-like effect of celocoxib Piroxicam in rat models of depression, J. Neural Transm. 121 (2014) 671–682.
[11] D.D. Stevenson, Adverse reactions to nonsteroidal anti-inflammatory drugs, Immunol. Allergy Clin. 18 (1998) 773–798.
[12] M.M. Wolfe, D.R. Lichtenstein, G. Singh, Gastrointestinal toxicity of nonsteroidal anti-inflammatory drugs, N. Engl. J. Med. 340 (1999) 1888–1899.
[13] S.K. Yadav, B. Adhikary, S.K. Bandyopadhyay, S. Chattopadhyay, Inhibition of TNF-α, and NF-κB and JNK pathways accounts for the prophylactic action of the natural phenolic, allylpyrocatechol against indomethacin gastropathy, Biochim. Biophys. Acta 1830 (2013) 3776–3786.

[14] E. Touraud, B. Roig, J.P. Sumpter, C. Coetsier, Drug residues and endocrine disruptors in drinking water: risk for humans? Int. J. Hyg. Environ. Health 214 (2011) 437–441.
[15] F. Méndez-Arriaga, S. Esplugas, J. Giménez, Photocatalytic degradation of non-steroidal anti-inflammatory drugs with TiO_2 and simulated solar irradiation, Water Res. 42 (2008) 585–594.
[16] M. Passananti, M. Lavorgna, M.R. Iesce, M. Della Greca, M. Brigante, E. Criscuolo, F. Cermola, M. Isidor, Photochemical fate and eco-genotoxicity assessment of the drug etodolac, Sci. Total Environ. 518–519 (2015) 258–265.
[17] J. Rivera-Utrilla, M. Sánchez-Polo, M.Á. Ferro-García, G. Prados-Joya, R. Ocampo-Pérez, Pharmaceuticals as emerging contaminants and their removal from water. A review, Chemosphere 93 (2013) 1268–1287.
[18] P. Van Antwerpen, J. Nève, In vitro comparative assessment of the scavenging activity against three reactive oxygen species of non-steroidal anti-inflammatory drugs from the oxicam and sulfoanilide families, Eur. J. Pharmacol. 496 (1–3) (2004) 55–61.
[19] E. Lemp, G. Günther, S.A. Zanocco, Sensitized photooxygenation of piroxicam in neat solvents and solvent mixtures, J. Photochem. Photobiol. B Biol. 65 (2001) 165–170.
[20] G. Günther, S.E. Lemp, A. Zanocco, Determination of chemical rate constants in singlet molecular oxygen reactions by using 1,4-dimethylnaphthalene endoperoxide, J. Photochem. Photobiol. A Chem. 151 (2002) 1–5.
[21] R.R. Yettella, D.B. Min, Effects of Trolox and ascorbic acid on the riboflavin photosensitised oxidation of aromatic amino acids, Food Chem. 118 (2010) 35–41.
[22] D. Vione, P.R. Maddigapu, E. De Laurentiis, M. Minella, M. Pazzi, V. Maurino, C. Minero, S. Kouras, C. Richard, Modelling the photochemical fate of ibuprofen in surface waters, Water Res. 45 (2011) 6725–6736.
[23] P.G. Tratnyek, J. Hoigné, Oxidation of substituted phenols in the environment: a QSAR analysis of rate constants for reaction with singlet oxygen, Environ. Sci. Technol. 25 (1991) 1596–1604.
[24] S. Criado, S.G. Bertolotti, A.T. Soltermann, N.A. García, Kinetic studies of the photosensitized oxidation ($O_2(^1\Delta g)$-mediated) of tryptophan-alkyl esters in Triton X-100 micellar solutions, J. Photochem. Photobiol. B Biol. 38 (1997) 107–113.
[25] R. Banerjee, H. Chakraborty, M. Sarkar, Photophysical studies of oxicam group of NSAIDs: piroxicam, meloxicam and tenoxicam, Spectrochim. Acta A 59 (6) (2003) 1213–1222.
[26] D. Ivanova, V. Deneva, D. Nedeltcheva, F.S. Kamounah, G. Gergov, P.E. Hansen, S. Kawauchi, L. Antonov, Tautomeric transformations of piroxicam in solution: a combined experimental and theoretical study, RSC Adv. 5 (2015) 31852–31860.
[27] D. Rodríguez-Barrientos, A. Rojas-Hernandez, A. Gutierrez, R. Moya-Hernández, R. Gómez-Balderas, M.T. Ramírez-Silva, Determination of pKa values of tenoxicam from ^{1}H NMR chemical shifts and of oxicams from electrophoretic mobilities (CZE) with the aid of programs SQUAD and HYPNMR, Talanta 80 (2) (2009) 754–762.
[28] E. Sikorska, I. Khmelinskii, A. Komasa, J. Koput, L.F.V. Ferrerira, J.R. Herance, J.L. Bourdelande, S.C.X. Williams, D.R. Worral, M. Insisnka-Rak, M. Sirkorski, Spectroscopy and photophysics of riboflavin and iso-(6,7)-riboflavin, Chem. Phys. 314 (2005) 239–247.
[29] P.F. Heelis, The photophysical and photochemical properties of flavins (isoalloxazines), Chem. Soc. Rev. 11 (1982) 15–39.
[30] W. Massad, S.G. Bertolotti, M. Romero, N.A. Garcia, A kinetic study on the inhibitory action of sympathomimetic drugs towards photogenerated oxygen active species. The case of phenylephrine. J. Photochem. Photobiol. B Biol. 80 (2005) 130–138.
[31] J.N. Chacón, J. McLearie, R.S. Sinclair, Singlet oxygen yields and radical contributions in the dye-sensitized photo-oxidation in methanol of esters of polyunsaturated fatty acids (oleic, linoleic, linolenic and arachidonic), Photochem. Photobiol. 47 (1988) 647–656.
[32] C.M. Krishna, S. Uppuluri, P. Riesz, J.S. Zigler, D. Balasubramanian, A study on the photolysis efficiencies of some eye lens constituents, Photochem. Photobiol. 54 (1991) 51–58.
[33] E. Silva, A.M. Edwards, D. Pacheco, Visible light-induced photooxidation of gluocose sensitized by riboflavin, J. Nutr. Biochem. 10 (1999) 181–185.
[34] S.Y. Kim, O.J. Kwon, J.-W. Park, Inactivation of catalase and superoxide dismutase by singlet oxygen derived from photoactivated dye, Biochimie 83 (2001) 437–444.
[35] F. Wilkinson, W.P. Helman, A.B. Ross, Rate constants for the decay and reactions of the lowest electronically excited state of molecular oxygen in solution. An extended and revised compilation. J. Phys. Chem. Ref. Data 24 (1995) 663–1021.
[36] F. Wilkinson, W.P. Helman, A.B. Ross, Quantum yields for the photosensitized formation of the lowest electronically excited state of molecular oxygen in solution, J. Phys. Chem. Ref. Data 22 (1993) 114–275.
[37] R.C. Straight, J.D. Spikes, Photosensitized oxidation of biomolecules, in: A.A. Frimer (Ed.), Singlet O_2, 4, CRC Press, Boca Raton, FL 1985, pp. 91–143.
[38] M. Koizumi, S. Kato, N. Mataga, T. Matsuura, I. Isui, Photosensitized Reactions, Kagakudogin Publishing Co, Kyoto, Japan, 1978.
[39] A. Radi, M.A. El Ries, F. El-Anwar, Z. El-Sherif, Electrochemical oxidation of meloxicam and its determination in tablet dosage form, Anal. Lett. 34 (5) (2001) 739–748.
[40] D.S. Guzman-Hernandez, M.T. Ramirez-Silva, M. Palomar-Pardave, S. Corona-Avendaño, A. Galano, A. Rojas-Hernandez, M. Romero-Romo, Electrochemical characterization of tenoxicam using a bare carbon paste electrode under stagnant and forced convection conditions, Electrochim. Acta 59 (2012) 150–155.
[41] A.A.J. Torriero, C.E. Tonn, L. Sereno, J. Raba, Electrooxidation mechanism of non-steroidal anti-inflammatory drug piroxicam at glassy carbon electrode, J. Electroanal. Chem. 588 (2006) 218–225.
[42] G. Porcal, S.G. Bertolotti, C.M. Previtali, M.V. Encinas, Electron transfer quenching of singlet and triplet excited states of flavins and lumichrome by aromatic and aliphatic electron donors, Phys. Chem. Chem. Phys. 5 (2003) 4123–4128.
[43] I.B. Afanas'ev, Superoxide Ion: Chemistry and Biological Implications, vol. ICRC Press, Boca Ratón. FL, 1989.
[44] N.A. García, Singlet molecular oxygen mediated photodegradation of aquatic phenolic pollutants. A kinetic and mechanistic overview, J. Photochem. Photobiol. B Biol. 22 (1994) 185–196.
[45] P.F. Heelis, The photochemistry of flavins, in: F. Müller (Ed.), Chemistry and Biochemistry of Flavoenzymes, vol. 1, CRC Press, Boca Ratón, FL 1991, p. 171.
[46] H. Görner, Oxygen uptake after electron transfer from amines, amino acids and ascorbic acid to triplet flavins in air-saturated aqueous solution, J. Photochem. Photobiol. B Biol. 87 (2007) 73–80.
[47] A. Momzikoff, R. Santus, M. Giraud, A study of the photosensitizing properties of seawater, Mar. Chem. 12 (1983) 1–14.